

## Adiabatic stabilization of excitons in an intense terahertz laser

Ren-Bao Liu and Bang-Fen Zhu

Center for Advanced Study, Tsinghua University, Beijing 100 084, People's Republic of China

(Received 11 April 2002; published 8 July 2002)

Calculation of near-infrared absorption and transient spectra in bulk semiconductors irradiated by an intense terahertz (THz) laser predicts that, the ionization rate of the ground-state exciton, probed through the dynamic Fano resonance effect may decrease with the increase of the THz laser intensity. This counterintuitive effect indicates the excitons are stabilized against the field ionization. The much lower Rydberg energy and “atomic unit” of laser intensity for excitons and, in particular, the possibility of creating excitons from the “vacuum state” in semiconductors allow observing the excitonic stabilization experimentally, in contrast to the case of atomic stabilization.

DOI: 10.1103/PhysRevB.66.033106

PACS number(s): 78.30.Fs, 32.80.Fb, 42.50.Md, 71.35.Cc

In accordance to Einstein's theory of the photoelectric effect, an electron can be stripped from its atom by light beams with sufficiently high frequency. As the intensity of a light beam is increased, the stripping probability of the electron increases owing to the increasing number of photon impacts. Surprisingly, since the late 1980s, theoretical investigations and numerical simulations<sup>1–6</sup> have predicted that when the electric field, associated with a laser of sufficiently high intensity and frequency, approaches or exceeds the electrostatic field between the electron and the ion in an atom, the wave function of the irradiated atom may be distorted adiabatically into a distribution with two well separated peaks. The peak spacing increases with increasing field intensity, thus the atomic electron spends more time far away from the nucleus, and the ionization rate slows down dramatically till almost totally suppressed. In other words, the adiabatic stabilization of the atom occurs.

Apart from the pure curiosity in basic research, the atomic stabilization is also of importance in potential application, such as the high harmonic generation<sup>7</sup> and quantum computation,<sup>8</sup> as it can quench the undesired ionization and dephasing caused by the intense laser that is used to drive electrons or to manipulate a qubit in an atom.

However, it is still controversial whether the adiabatic atomic stabilization is an experimentally observable effect.<sup>9,10</sup> Basically, the objection is based on the fact that the turnon of the laser pulse must be sufficiently slow in order to adiabatically drive a bare atomic ground-state into a quasi-stationary dressed state; while substantial ionization has already been inevitable during the ramp of the intense laser pulse.<sup>11</sup> In addition to this fundamental difficulty mentioned above, an extreme ultraviolet laser with intensity stronger than an atomic unit ( $\sim 3.51 \times 10^{16}$  W/cm<sup>2</sup>) required for the atomic stabilization, seems unavailable in the near future. In fact, except for a few disputable indications for the stabilization of high Rydberg states,<sup>12</sup> so far there is no unambiguous experimental evidence for the atomic stabilization.

In this paper, we predict the adiabatic stabilization of hydrogen-atom-like excitons in semiconductors, which might settle the debate around the atomic stabilization effect mentioned above. We demonstrate that the excitonic stabilization (XS), in contrast to its atomic counterpart, is definitely an observable effect, owing to the basic characteristic of ex-

citons that they are created from “vacuum” of carriers by the interband optical excitation. In particular, we proposed the dressed exciton states to be prepared by weak near-infrared (NIR) laser pulses in semiconductors in the presence of a quasicontinuous terahertz (THz) field. The ionization rate or lifetime of the dressed excitons can be directly extracted by monitoring either the linewidth of absorption peaks or the decay time of transient signals. Thus the “turnon” problem is circumvented as long as the pulsed interband excitation and the following dephasing process of excitons are covered by the flat-top region of the THz laser pulse.

Moreover, the present laboratory gear is already ready for observing the XS effect. Due to the small effective mass  $\mu$  and large dielectric constant  $\epsilon$ , an exciton has much smaller binding energy  $E_B$  than the hydrogen atom does, and the “excitonic unit” for laser intensity ( $\propto \mu^4/\epsilon^{5.5}$ ) in a typical semiconductor like GaAs is about 10 orders of magnitude smaller than the atomic unit. So, the “high-intensity and high-frequency” requirement for the XS can readily be fulfilled by the free-electron lasers operating with MW/cm<sup>2</sup> power and THz frequency.<sup>13</sup>

The XS, manifesting itself as the line narrowing and quench of the dephasing, is also a novel effect of a strong ac field on exciton dynamics in semiconductors. Though several novel effects, referred to as the dynamic Franz-Keldysh effect,<sup>14–16</sup> have already been explored recently, such as the excitonic ionization,<sup>14</sup> excitonic blueshift,<sup>15</sup> sideband generation,<sup>16–18</sup> absorption in the band gap,<sup>17</sup> and inter-sideband quantum interference,<sup>18,19</sup> this is still a developing field.

Our investigation is based on the numerical solution of the motion equation for the relative motion of an electron-hole pair within the effective-mass approximation

$$i\hbar \partial_t \psi(\mathbf{r}, t) = (\hat{H} - i\gamma_2) \psi(\mathbf{r}, t) + \chi(t) e^{-i\Omega_0 t} \delta(\mathbf{r}), \quad (1)$$

$$\hat{H} \equiv E_g - \frac{\hbar^2}{2\mu} \nabla_{\mathbf{r}}^2 - \frac{e^2}{4\pi\epsilon r} + eFz \cos(\omega t), \quad (2)$$

where  $E_g$  is the band gap,  $F$  is the field strength of the THz laser associated with frequency  $\omega$  and linearly polarized in the  $\mathbf{z}$  direction,  $\chi(t)$  denotes the NIR pulse excitation centered at  $\Omega_0$ , and  $\gamma_2$  is an interband dephasing rate due to

phonon scattering. The THz laser is assumed in a continuous wave (cw) form, because its microsecond duration<sup>13</sup> is much longer than the picosecond interband excitation and dephasing process. This model system is mathematically equivalent to a hydrogen atom in an intense laser except that the electron-hole pair is generated by the NIR laser.

Without the Coulomb coupling, the eigensolution of the time-dependent Hamiltonian [Eq. (2)] is the Volkov state,<sup>20</sup> which, as the basis set, reads

$$|\mathbf{k}, m\rangle = e^{im\omega t - ia_F k_z \cos(\omega t) + i(U_p/2\hbar\omega)\sin(2\omega t)} |\tilde{\mathbf{k}}\rangle,$$

where  $m$  and  $\mathbf{k}$ , associated with quasienergy  $\varepsilon_{\mathbf{k}m} = (\hbar^2 k^2)/2\mu + U_p + m\hbar\omega$ , denote the sideband index and wave vector, respectively. Here  $U_p \equiv (e^2 F^2)/(4\mu\omega^2)$  is the effective ponderomotive potential,  $a_F \equiv (eF)/(\mu\omega^2)$  is the classical excursion amplitude of an electron in the THz field, and  $|\tilde{\mathbf{k}}\rangle$  is the Bloch state with accelerating quasimomentum  $\mathbf{k} - (eF)/(\hbar\omega)\hat{z}\sin(\omega t)$ . With the excitonic Rydberg unit adopted, the matrix elements of the Coulomb potential read

$$V_{\mathbf{k}+\mathbf{q}m+n, \mathbf{k}m} = -\pi^{-2} q^{-2} i^n J_n(a_F q_z),$$

where  $J_n(x)$  denotes the  $n$ th-order Bessel function of the first kind. The intra-sideband ( $n=0$ ) interaction is directly related to the Kramers-Hennerberg (KH) potential, the time-average of the Coulomb potential in the coordinate frame rested on the quivering electron.<sup>21</sup> The KH potential has logarithmic singularity in the segment between the turning points  $\pm \hat{z}a_F$  and  $r^{-1/2}$  singularity at the ends. Consequently, the ground state  $|\Phi\rangle$  is stretched along the segment of singularity and becomes dichotomous for superintense field ( $a_F \gg a_B$ , the exciton Bohr radius).<sup>1</sup>

The spectrum of the system exhibits the sideband structure. As illustrated in the lower inset in Fig. 1, each sideband consists of several discrete states and a continuum, and the discrete states are embedded in the ionization continua of lower sidebands. As predicted very recently in an ac-driven biased semiconductor superlattice,<sup>19</sup> the quantum interference between a discrete state of quasienergy excitons and the degenerate continuum of a sideband can lead to the dynamic Fano resonance (DFR), which manifests itself as broadened asymmetric lineshape in absorption spectra and as intrinsic decay in transient four-wave mixing signals. Thus, the ionization rate of the quasibound Floquet-state excitons and the XS effect can be studied via the DFR induced by the inter-sideband coupling ( $n \neq 0$ ) in the present system.

To calculate the time-dependent wave function, we numerically integrate Eq. (1) in the cylindrical polar coordinates by extending the space-time difference method<sup>22</sup> to a time-periodic system, with the initial condition as  $\psi(\mathbf{r}, -\infty) = 0$ . The outgoing waves are absorbed at the boundary with the mask technique.<sup>4</sup> The NIR absorption spectrum  $\alpha(\Omega) \propto \mathcal{J}[P(\Omega)/\chi(\Omega)]$ , in which  $P(t) \equiv \psi(\mathbf{0}, t)$ , gives directly the transient interband polarization (i.e., coherence). Our real-space method is able to include the Coulomb interaction, the nonperturbative ac field, and the contribution

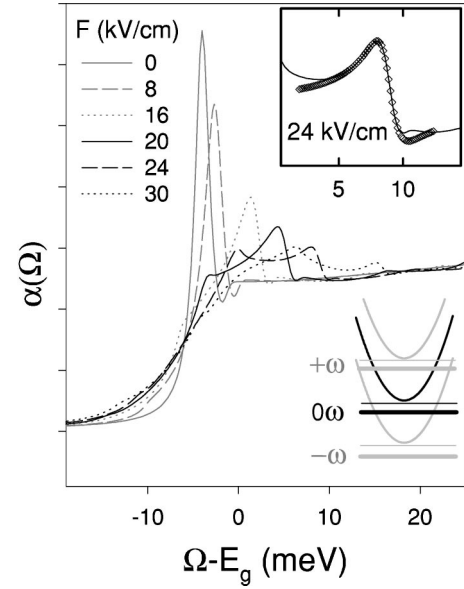


FIG. 1. Linear absorption spectrum for several THz-field strengths indicated by  $F$ . The upper-right inset shows, as an example, the Fano resonance fitting process for  $F = 24$  kV/cm, where the squares are the fitted data. The lower-right inset shows schematically the sideband structure of the Floquet-state excitonic spectrum.

of continuum states properly, so as to correctly work out the spectral features with high resolution. In the calculation,  $\hbar\omega = 10$  meV ( $\sim 2.4$  THz),  $\gamma_2 = 1$  meV, and the NIR pulse is assumed to be of a Gaussian shape, i.e.,  $\chi(t) = \chi_0 \exp(-t^2/2\tau^2)$ . For cw absorption,  $\tau$  is taken as  $8/\omega$ , which is large enough to eliminate the sideband overlap. The material parameters take bulk GaAs as an example ( $E_B = 4$  meV and  $a_B = 10$  nm).

Figure 1 plots the NIR cw-absorption spectra of the bulk GaAs driven by the THz field with various strength. The exciton ionization rate is probed through the broadening and distortion of absorption peaks in the NIR spectra. As displayed in the inset, the asymmetric resonance peak is well fitted with the Fano lineshape<sup>23</sup> characterized by the shape parameter  $q$  and broadening constant  $\gamma$ ,

$$\alpha(\Omega) = \alpha_0 + \alpha_1 \frac{(q\gamma + \Omega - E_g + \mathcal{E}_B)^2}{\gamma^2 + (\Omega - E_g + \mathcal{E}_B)^2},$$

indicating the occurrence of the DFR ( $\mathcal{E}_B$  is the binding energy of the dressed exciton state). By fitting the  $0\omega$  (i.e., zero-THz-photon-assisted)  $1s$  exciton peak, the ionization rate  $\Gamma$  can be extracted via  $\gamma \approx \gamma_2 + \Gamma/2$ . As shown in Fig. 2,  $\gamma$  (hence the ionization rate) increases with the laser intensity until  $F \approx 16$  kV/cm [corresponding to the intensity  $I \approx 1.0$  MW/cm<sup>2</sup> (Ref. 24) and  $a_F \approx 1.28a_B$ ]. Beyond that critical field strength, the ionization rate commences to decrease, and approaches zero at  $F \approx 28$  kV/cm, clearly demonstrating the XS effect. The ionization rate extracted from

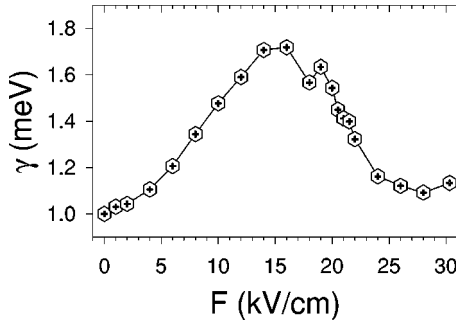


FIG. 2. Fano broadening constant deduced from the DFR versus the THz-field strength.

the DFR, after energy scaling, is consistent with that obtained in atomic physics by directly diagonalizing the Floquet-state Hamiltonian.<sup>5</sup>

$\Gamma$  can also be obtained analytically in the high-frequency approximation.<sup>25</sup> When the wave-function dichotomy is negligible for medium  $a_F$  (say  $a_F < 3a_B$ ), a compact result for  $\Gamma$  of the ground state<sup>25</sup> can be derived as

$$\Gamma \approx \sum_{n\omega > \mathcal{E}_B} \frac{32\pi}{k_n^3} \left| \int_{-a_F}^{+a_F} \frac{\Phi(\mathbf{z})dz}{2a_F} \right|^2 \int_0^1 J_n^2(a_F k_n x) dx,$$

where  $k_n^2 = n\omega - \mathcal{E}_B$ . As implied by the two integrals in the equation above, two main mechanisms are responsible for the XS. First, the stretch of the excitonic wave function by the intense THz field reduces the electron-hole overlap and hence the probability of scattering. Second, the stretch of the wave function induces interference cancellation between outgoing waves scattered at different positions (similar to the case of light diffraction by a single slit, where the wider the slit, the denser the diffraction fringes.)

Fano interference is one of fundamental mechanisms for irreversible decay,<sup>26,27</sup> so the XS can also be directly observed in the time domain by monitoring the transient optical signal after a pulsed excitation. The time-resolved interband polarization is plotted in Fig. 3. The duration of the NIR pulse  $\tau$  is then set to be  $2/\omega$ , and the central frequency is chosen for each field strength to be resonant with the brightest transition, namely,  $\Omega_0 - E_g = -4, -2, 2, 5,$  and  $6$  meV for  $F=0, 8, 16, 20,$  and  $30$  kV/cm, respectively. To single out the dephasing induced by the DFR only, the reformulated signal  $\mathcal{P}(t) \equiv P(t)\exp(\gamma_2 t)$  is plotted. The dynamic Fano interference between the discrete state and the continuum opens a new channel for interband dephasing, leading to the decay of the transient signal. The XS effect is verified by the fact that the dephasing rate calculated begins to decrease for  $F > 16$  kV/cm, consistent with the variation trend of the ionization rate as shown in Fig. 2. When  $F=30$  kV/cm [ $I \approx 3.6$  MW/cm<sup>2</sup> (Ref. 24)], the decay of the signal almost disappears. To measure the transient signals, nonlinear optical experiments like four-wave mixing are usually adopted, in which many-body correlation is important sometimes<sup>28</sup> and may induce new interesting effects on XS, which, however, is out of the scope of our present study.

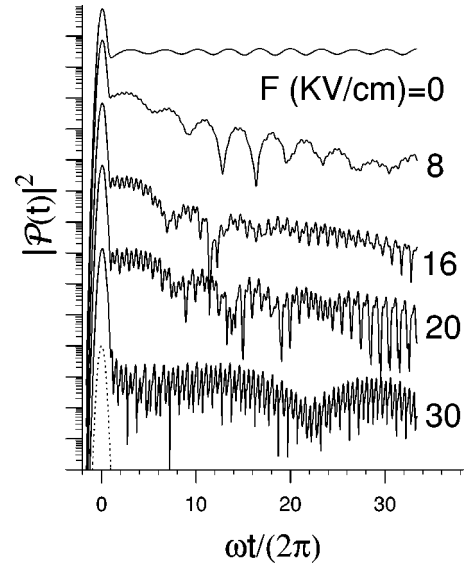


FIG. 3. Real-time dependence of the interband polarization for various THz-field strength indicated by  $F$ , in which the curves are offset for clarity. The intensity profile of the NIR pulse (the dotted curve) is also shown for comparison.

Figure 4 displays snapshots of the probability distribution of the exciton wavepacket resonantly excited by a pulse ( $\Omega_0 - E_g = 8.88$  meV) with  $\tau = 20/\omega$  (the excitation spectrum width is 0.5 meV). When the NIR-excitation pulse is over, a stabilized wave packet performs almost perfect periodic swinging along the  $z$  axis with the turning points located at about  $\pm \hat{z}a_F$ . Along with the periodic variation of the wave-packet shape due to the nondegenerate inter-sideband mixing, the stretch of the wave function can be observed. A closer examination reveals the interference pattern of the scattered waves. All these justify our ascribing the suppres-

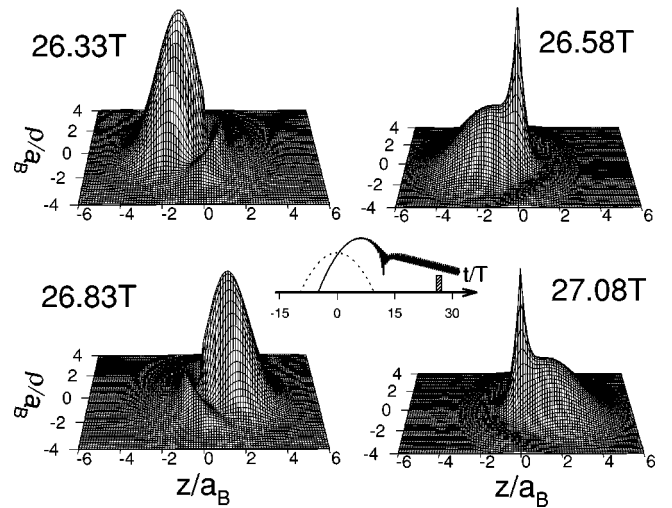


FIG. 4. Probability distribution of the NIR-pulse-excited wave packet at several time instant within a period  $T \equiv 2\pi/\omega$  for the THz field of  $F=24$  kV/cm. The inset shows the semilogarithmic plots of the intensity of the NIR pulse (dotted line) and transient interband optical signal ( $|\mathcal{P}(t)|^2$ , solid line) as functions of time, and the time snatch (marked by the bar) where the snapshots are made.

sion of the Fano broadening and dephasing rate to the adiabatic XS, and demonstrate that the stabilized exciton can be excited by an additionally NIR laser.

In summary, the novel excitonic stabilization effect has been predicted in a coupled system of semiconductors and intense THz fields by nonperturbative numerical simulation. The excitonic stabilization is fundamentally different from

its atomic counterpart in that the stabilized exciton is an elementary excitation in solids and hence can be excited by a NIR laser.

This work was supported by the National Science Foundation of China, and R.B.L was also supported by China Postdoctoral Science Foundation.

- 
- <sup>1</sup>M. Pont, N.R. Walet, M. Gavrilă, and C.W. McCurdy, *Phys. Rev. Lett.* **61**, 939 (1988); M. Pont, N.R. Walet, and M. Gavrilă, *Phys. Rev. A* **41**, 477 (1990).
- <sup>2</sup>M. Pont and M. Gavrilă, *Phys. Rev. Lett.* **65**, 2362 (1990).
- <sup>3</sup>Q. Su, J.H. Eberly, and J. Javanainen, *Phys. Rev. Lett.* **64**, 862 (1990).
- <sup>4</sup>K.C. Kulander, K.J. Schafer, and J.L. Krause, *Phys. Rev. Lett.* **66**, 2601 (1991).
- <sup>5</sup>M. Dörr, R.M. Potvliege, D. Proulx, and R. Shakeshaft, *Phys. Rev. A* **43**, 3729 (1991).
- <sup>6</sup>J.H. Eberly and K.C. Kulander, *Science* **262**, 1229 (1993).
- <sup>7</sup>P. Salières, A. L'Huillier, P. Antoine, M. Lewenstein, in *Advances in Atomic, Molecular, and Optical Physics*, edited by B. Bederson and H. Walther (Academic Press, New York, 1999), Vol. 41, p. 83.
- <sup>8</sup>B.E. Cole, J.B. Williams, B.T. King, M.S. Sherwin, and C.R. Stanley, *Nature (London)* **410**, 60 (2001).
- <sup>9</sup>S. Geltman, *Chem. Phys. Lett.* **237**, 286 (1995).
- <sup>10</sup>C. Figueira de Morisson Faria, A. Fring, and R. Schrader, *J. Phys. B* **31**, 449 (1998).
- <sup>11</sup>P. Lambropoulos, *Phys. Rev. Lett.* **55**, 2141 (1985).
- <sup>12</sup>M.P. de Boer, J.H. Hoogenraad, R.B. Vrijen, L.D. Noordam, and H.G. Muller, *Phys. Rev. Lett.* **71**, 3263 (1993); N.J. van Druten, R.C. Constantinescu, J.M. Schins, H. Nieuwenhuize, and H.G. Muller, *Phys. Rev. A* **55**, 622 (1997).
- <sup>13</sup>G. Ramian, *Nucl. Instrum. Methods Phys. Res. A* **318**, 225 (1992).
- <sup>14</sup>J. Cêrne, J. Kono, M.S. Sherwin, M. Sundaram, A.C. Gossard, and G.E. Bauer, *Phys. Rev. Lett.* **77**, 1131 (1996).
- <sup>15</sup>K.B. Nordstrom, K. Johnsen, S.J. Allen, A.-P. Jauho, B. Bimir, J. Kono, T. Noda, H. Akiyama, and H. Sakaki, *Phys. Rev. Lett.* **81**, 457 (1998).
- <sup>16</sup>J. Kono, M.Y. Su, T. Inoshita, T. Noda, M.S. Sherwin, S.J. Allen, Jr., and H. Sakaki, *Phys. Rev. Lett.* **79**, 1758 (1997).
- <sup>17</sup>A.P. Jauho and K. Johnsen, *Phys. Rev. Lett.* **76**, 4576 (1996).
- <sup>18</sup>A.V. Maslov and D.S. Citrin, *Phys. Rev. B* **62**, 16 686 (2000).
- <sup>19</sup>R.B. Liu and B.F. Zhu, *J. Phys.: Condens. Matter* **12**, L741 (2000).
- <sup>20</sup>D.M. Volkov, *Z. Phys.* **94**, 250 (1935).
- <sup>21</sup>H. A. Kramers, *Collected Scientific Papers* (North-Holland, Amsterdam, 1956), p. 866; W.C. Henneberger, *Phys. Rev. Lett.* **21**, 838 (1968).
- <sup>22</sup>S. Glutsch, D.S. Chemla, and F. Bechstedt, *Phys. Rev. B* **54**, 11 592 (1996).
- <sup>23</sup>U. Fano, *Phys. Rev.* **124**, 1866 (1961).
- <sup>24</sup>Here we use the intensity inside the material with relative dielectric constant  $\varepsilon/\varepsilon_0=9.0$ . The vacuum value is larger by about 1.3.
- <sup>25</sup>M. Pont, *Phys. Rev. A* **44**, 2141 (1991); **44**, 2152 (1991).
- <sup>26</sup>U. Siegner, M.-A. Mycek, S. Glutsch, and D.S. Chemla, *Phys. Rev. Lett.* **74**, 470 (1995).
- <sup>27</sup>C.P. Holfeld, F. Löser, M. Sudzius, K. Leo, D.M. Whittaker, and K. Köhler, *Phys. Rev. Lett.* **81**, 874 (1998).
- <sup>28</sup>D.S. Chemla and J. Shah, *Nature (London)* **411**, 549 (2001).